ELSEVIER

International Journal of Solids and Structures 41 (2004) 2899–2917

INTERNATIONAL JOURNAL OF SOLIDS and STRUCTURES

www.elsevier.com/locate/ijsolstr

Orthotropic rescaling for crack tip fields in linear piezoelectric materials

Christopher S. Lynch *, William S. Oates

The GWW School of Mechanical Engineering, The Georgia Institute of Technology, 801 Ferst Dr. NW MRDC, Atlanta, GA 30332-0405, USA

Received 5 December 2003; received in revised form 5 December 2003

Available online 3 March 2004

Abstract

Analysis of stress fields in a linear elastic–piezoelectric–dielectric medium requires use of anisotropic elasticity theory. Many researchers employ the Stroh formalism, which requires the solution of a sixth order characteristic equation involving material coefficients. This equation must be solved numerically for each material composition to obtain the eigenvalues and eigenvectors that give the resulting field quantities. The focus of this work is the development of a closed form solution for the electro-mechanical crack tip fields in piezoelectric materials using orthotropic rescaling to reduce the governing field equations to the biharmonic equation and the Poisson equation. Solutions for an isotropic linear elastic material are utilized to obtain solutions for the anisotropic piezoelectric material. This leads to closed form solutions for the fields in terms of ratios of certain elastic, dielectric, and piezoelectric coefficients. Orthotropic rescaling and the Stroh formalism are compared and recommendations are made for when and when not to use the orthotropic rescaling approach.

Keywords: Stroh's formalism; Orthotropic rescaling; Piezoelectric; Anisotropic fracture

1. Introduction

The reliability of piezoelectric materials is of interest due to their abundant applications in smart systems and structures. Devices which implement piezoelectric materials include active vibration dampers, mirror positioners, accelerometers, micropumps, and fuel injectors. Although these materials have considerable technological capabilities, they are limited by fatigue and fracture.

Recent work in the area of fracture mechanics has been focused on determining crack tip fields in anisotropic piezoelectric materials. The coupled electro-mechanical behavior poses a challenge in obtaining closed form solutions that describe the field quantities. Ting (1996) has described the Stroh formalism in

* Corresponding author. Tel.: +1-404-894-6871; fax: +1-404-894-0186.
E-mail addresses: chris.lynch@me.gatech.edu, lynch.admin@me.gatech.edu (C.S. Lynch).

0020-7683/$ - see front matter © 2004 Elsevier Ltd. All rights reserved.
doi:10.1016/j.ijsolstr.2004.01.010

detail for elastic materials. This technique has been extended to piezoelectric materials by Suo et al. (1992), Pak (1992), McMeeking (1999), and Zhang et al. (2001). Sosa (1990) used a similar technique by determining a general solution in terms of complex potentials.

Stroh's formalism makes use of an eigenvector problem that is developed by applying mechanical equilibrium and charge compatibility to the constitutive equations. A vector potential representing displacement and electric potential is assumed. This automatically satisfies strain compatibility and curl-free electric field, but involves solving an eigenvector problem that requires the solution of a sixth order polynomial for each material composition. This makes it very difficult to ascertain the role of material anisotropy in the fracture process.

A different approach is presented here that explicitly solves the field equations in terms of material coefficients using a modified orthotropic rescaling approach. Suo et al. (1991) determined the stress fields in elastic composite materials by employing orthotropic rescaling. In orthotropic elastic solids, the coordinate axes can be rescaled to obtain the biharmonic equation when a certain ratio of elastic coefficients is unity. For piezoelectric materials, one additional constraint is necessary. A specific ratio of piezoelectric and dielectric coefficients decouples the mechanical and electrical terms. When this decoupling ratio is realized and the biharmonic equation is attained, closed form solutions for the stress components can be determined. The decoupling coefficient is then utilized to determine the electrical components by solving the Poisson equation.

The first part of this work summarizes the governing equations and general solutions to the coupled piezoelectric problem for the two approaches. In the orthotropic rescaling, the rescaling technique and decoupling coefficients are determined which lead to the biharmonic equation and the Poisson equation in the rescaled coordinate system. A brief review of Stroh's formalism is given with emphasis on the relation between the Stroh complex potentials and the potentials used in the orthotropic rescaling.

The second part of the work applies the orthotropic rescaling and the Stroh formalism technique to the crack problem in an infinite piezoelectric medium. The two solution techniques are shown to be in exact agreement when specific ratios of the material coefficients hold. Actual material properties are then applied and deviations in the predicted stress fields near the crack tip are addressed. A parametric study is conducted to determine the effect of variations in the decoupling coefficient on the maximum principal stress near the crack tip.

2. Governing equations

The governing equations are presented in indicial notation, with summation implied over repeated indices. The small strain assumption is used since the results are to be applied to piezoelectric ceramics and crystals that strain less than 1%. The effect of a polar medium inducing a non-symmetric stress tensor is neglected. Kamlah (2001) showed that the stress induced by the polarity of the medium is on the order of 1 MPa, negligible relative to the far higher stresses found in the elastic problem. Under these assumptions, the following field equations govern linear piezoelectric solids.

Mechanical equilibrium of stress is given by the divergence of the second order stress tensor when body forces are negligible.

$$\sigma_{ji,j} = 0 \tag{2.1}$$

The mechanical equilibrium equation is satisfied when the stress is given by the double curl of a second order potential,

$$\sigma_{ij} = -\Phi_{mn,kl} \in_{ikm} \in_{jnl} \tag{2.2}$$

where Φ_{ij} is the second order stress potential and $\in_{pki}$ is the components of the permutation symbol (Weber, 1948). For two-dimensional problems, the second order stress potential reduces to the Airy stress potential given by Eq. (2.3).

$$\Phi = \Phi_{33}(x_1, x_2) \tag{2.3}$$

In this case the stress field is represented by the following equation,

$$\sigma_{ij} = \Phi_{,kk}\delta_{ij} - \Phi_{,ij} \tag{2.4}$$

where δ_{ij} is the Kronecker delta.

The small strain–displacement relation is given by

$$\varepsilon_{ij} = \tfrac{1}{2}(u_{i,j} + u_{j,i}) \tag{2.5}$$

where ε_{ij} is the strain and u_i is the displacement vector.

Compatibility conditions must hold to ensure three displacements can be determined from the six strain components. The compatibility condition is given by Eq. (2.6)

$$\in_{pki}\in_{mjl} \varepsilon_{ij,kl} = 0 \tag{2.6}$$

Quasi-static charge balance in the absence of free charge is given by

$$D_{i,i} = 0 \tag{2.7}$$

where D_i is the electric displacement vector.

Eq. (2.7) is satisfied when the electric displacement is found from the curl of a vector potential,

$$D_p = \Psi_{i,k} \in_{pki} \tag{2.8}$$

For two-dimensional problems, the electric displacement vector potential reduces to the following scalar potential,

$$\Psi_3 = \Psi_3(x_1, x_2) \tag{2.9}$$

In quasi-static problems the curl of the electric field is zero.

$$E_{i,k} \in_{pki} = 0 \tag{2.10}$$

This condition is satisfied when the electric field vector is represented by the gradient of the electric potential.

$$E_i = -\phi_{,i} \tag{2.11}$$

The coupled form of the electro-mechanical constitutive law can be written in several forms. The Stroh formalism typically uses the form given by Eqs. (2.12a,b).

$$\sigma_{ij} = C^E_{ijkl}\varepsilon_{kl} - e_{kij}E_k \tag{2.12a}$$

$$D_i = e_{ikl}\varepsilon_{kl} + \kappa^{\varepsilon}_{ik}E_k \tag{2.12b}$$

where C^E_{ijkl} are the stiffness coefficients at constant electric field, e_{kij} are the piezoelectric coefficients, and $\kappa^{\varepsilon}_{ik}$ are the dielectric coefficients at fixed strain.

The orthotropic rescaling technique may use one of two forms of the constitutive law given below,

$$\varepsilon_{ij} = s^E_{ijkl}\sigma_{kl} + d_{kij}E_k \tag{2.13a}$$

$$D_i = d_{ikl}\sigma_{kl} + \kappa^{\sigma}_{ik}E_k \tag{2.13b}$$

$$\varepsilon_{ij} = s^{D}_{ijkl}\sigma_{kl} + g_{kij}D_k \tag{2.14a}$$

$$E_i = -g_{ikl}\sigma_{kl} + \beta^{\sigma}_{ik}D_k \tag{2.14b}$$

where s^{D}_{ijkl} and s^{E}_{ijkl} are the open circuit and short circuit compliance coefficients, respectively, g_{kij} and d_{kij} are the piezoelectric coefficients, and β^{σ}_{ik} and κ^{σ}_{ik} are the dielectric impermittivity and permittivity coefficients at fixed stress, respectively.

Solutions to certain boundary value problems are more easily attained by satisfying traction and surface charge which are more readily applied using Eqs. (2.14a, b) and applying Eqs. (2.6) and (2.10). For example, the impermeable crack problem requires applying zero electric displacement normal to the crack face. This is achieved by using the electric displacement vector potential given by Eq. (2.8). If electric potential boundary conditions are preferred (such as a conducting crack which requires a zero electric potential across the crack face), the constitutive law given by Eqs. (2.13a, b) can be used by applying Eqs. (2.6) and (2.7).

Relations between the internal fields and the surface quantities are given by Eqs. (2.15) and (2.16).

$$t_i = \sigma_{ji}n_j \tag{2.15}$$

$$\omega = -D_i n_i \tag{2.16}$$

where t_i is the traction vector on the surface, n_j is a unit vector normal to the surface, and ω is the surface charge density. The mechanical displacement and the electric potential are continuous from the specified surface value to the material just beneath the surface. These boundary conditions will be used in solving the crack problem.

2.1. Material properties

The general solutions presented here using the orthotropic rescaling and the Stroh formalism technique focuses on two-dimensional problems. The determination of plane stress and plane strain field quantities requires decoupling the plane and anti-plane problems. For the case of the anisotropic elastic medium, symmetry in the elastic coefficients and a few minimal restrictions on the coefficients leads to uncoupled anti-plane and in-plane deformation (Ting, 1996). When considering plane problems, the in-plane displacements (u_1 and u_2) are only functions of the in-plane coordinates, x_1 and x_2, while the displacement perpendicular to the plane (u_3) is independent. Uncoupled anti-plane deformation requires the out of plane shear coupling elastic coefficients to be zero. Using Voigt notation (Malvern, 1969), the elastic shear coupling coefficients that must be zero are given by Eq. (2.17).

$$C_{14} = C_{15} = C_{24} = C_{25} = C_{46} = C_{56} = 0 \tag{2.17}$$

Poled piezoelectric ceramic materials and some piezoelectric single crystal cuts are transverse isotropic and no shear coupling exists; therefore, in-plane loading does not induce any anti-plane deformation. The non-zero elastic, piezoelectric and dielectric coefficients are given in Voight notation in Appendix A. A comment on notation: although the polarization direction is typically taken to be the x_3 direction in the piezoelectric literature, the two-dimensional problems discussed in the following sections take the polarization direction to be in the x_2 direction for consistency with the fracture mechanics literature. This requires a change of subscripts on all published piezoelectric material coefficients.

3. Orthotropic rescaling

The absence of shear coupling in transversely isotropic piezoelectric materials allows the orthotropic rescaling technique discussed by Suo et al. (1991) for elastic materials to be extended to piezoelectric materials. This class of piezoelectric materials (poled in the x_2 direction) has transverse isotropic symmetry about the poling axis.

3.1. Stress governing equations

The equations for the plane piezoelectric problem poled in the x_2 direction are developed assuming plane stress. The plane strain case requires some additional algebra to determine the material coefficients. This is done in Appendix A. The constitutive law governing strain, Eq. (2.12), is substituted into strain compatibility, Eq. (2.6), and reduced using the Airy stress function, Eq. (2.3), and the electric displacement potential, Eq. (2.9).

$$s^D_{1111}\Phi_{,2222} + 2(s^D_{1122} + 2s^D_{1212})\Phi_{,1122} + s^D_{2222}\Phi_{,1111} = (2g_{112} + g_{211})\Psi_{3,122} + g_{222}\Psi_{3,111} \tag{3.1}$$

The electric displacement potential terms in Eq. (3.1) must be eliminated using rescaling to further reduce Eq. (3.1) to the biharmonic equation governing the stress field in rescaled coordinates. The curl-free electric field is applied to Eq. (2.14b) and the result is used to eliminate these terms. It is expanded for the in-plane piezoelectric problem and given by Eq. (3.2).

$$-(g_{211} + 2g_{112})\Phi_{,122} - g_{222}\Phi_{,111} = \beta^\sigma_{11}\Psi_{3,22} + \beta^\sigma_{22}\Psi_{3,11} \tag{3.2}$$

A fourth order partial differential equation is obtained by differentiating Eq. (3.2) with respect to x_1. The resulting equation is then multiplied by a decoupling coefficient B.

$$B[-(g_{211} + 2g_{112})\Phi_{,1122} - g_{222}\Phi_{,1111} = \beta^\sigma_{11}\Psi_{3,122} + \beta^\sigma_{22}\Psi_{3,111}] \tag{3.3}$$

The electric displacement potential is eliminated by adding Eq. (3.3) to Eq. (3.1) and determining the necessary conditions to impose on the decoupling coefficient B. This gives Eq. (3.4).

$$\begin{aligned}&(s^D_{2222} - Bg_{222})\Phi_{,1111} + [2(s^D_{1122} + 2s^D_{1212}) - B(g_{211} + 2g_{112})]\Phi_{,1122} + s^D_{1111}\Phi_{,2222}\\ &\quad = (2g_{112} + g_{211} + B\beta^\sigma_{11})\Psi_{3,122} + (g_{222} + B\beta^\sigma_{22})\Psi_{3,111}\end{aligned} \tag{3.4}$$

The decoupling coefficient, B, must simultaneously satisfy two different conditions (typically exclusive), which are given by Eq. (3.5).

$$B = -\frac{(g_{211} + 2g_{112})}{\beta^\sigma_{11}} = -\frac{g_{222}}{\beta^\sigma_{22}} \tag{3.5}$$

The constraint given by Eq. (3.5) can be cast into the following ratio of piezoelectric and permittivity ratios.

$$\frac{\beta^\sigma_{11}}{\beta^\sigma_{22}} = \frac{g_{211} + 2g_{112}}{g_{222}} \tag{3.6}$$

When Eq. (3.6) is satisfied, a rescaling parameter can be introduced.

$$\tilde{x}_1 = x_1 \tag{3.7}$$

$$\tilde{x}_2 = ax_2 \tag{3.8}$$

where

$$\frac{\partial}{\partial x_1} = \frac{\partial}{\partial \tilde{x}_1}\frac{\partial \tilde{x}_1}{\partial x_1} = \frac{\partial}{\partial \tilde{x}_1} \tag{3.9}$$

and

$$\frac{\partial}{\partial x_2} = \frac{\partial}{\partial \tilde{x}_2}\frac{\partial \tilde{x}_2}{\partial x_2} = a\frac{\partial}{\partial \tilde{x}_2} \tag{3.10}$$

By using the rescaled coordinate system $(\tilde{x}_1, \tilde{x}_2)$, Eq. (3.4) is transformed to Eq. (3.11).

$$\Phi_{,1111} + a^2\left[\frac{2(s^D_{1122} + 2s^D_{1212}) - B(g_{211} + 2g_{112})}{s^D_{2222} - Bg_{222}}\right]\Phi_{,11\tilde{2}\tilde{2}} + \frac{a^4 s^D_{1111}}{s^D_{2222} - Bg_{222}}\Phi_{,\tilde{2}\tilde{2}\tilde{2}\tilde{2}} = 0 \tag{3.11}$$

To reduce Eq. (3.11) to the biharmonic equation in the rescaled coordinates, the rescaling parameter is defined as,

$$a^2 = \sqrt{\frac{s^D_{2222} - Bg_{222}}{s^D_{1111}}} \tag{3.12}$$

Substituting Eq. (3.12) into Eq. (3.11) gives

$$\Phi_{,1111} + 2\rho'\Phi_{,11\tilde{2}\tilde{2}} + \Phi_{,\tilde{2}\tilde{2}\tilde{2}\tilde{2}} = 0 \tag{3.13}$$

where

$$\rho' = \frac{2(s^D_{1122} + 2s^D_{1212}) - B(g_{211} + 2g_{112})}{2\sqrt{s^D_{1111}(s^D_{2222} - Bg_{222})}} \tag{3.14}$$

When $\rho' = 1$ Eq. (3.13) reduces to the biharmonic equation in the rescaled coordinates. This result allows previously determined elasticity solutions to be utilized to solve orthotropic piezoelectric problems. The factor, ρ', typically ranges between 0.77 and 1.31 for poled PZT materials. Numerical examples will be given which compare the "idealized" case, to real material coefficients by use of the Stroh formalism.

The rescaled governing equation is thus given by Eq. (3.15).

$$\nabla^4\Phi = 0 \tag{3.15}$$

To solve Eq. (3.15), the boundary conditions must be mapped into the $(\tilde{x}_1, \tilde{x}_2)$ coordinates. This will be addressed in Section 5.

3.2. Electrical field and electric displacement governing equations

The electrical components cannot be decoupled from the stress field. They must be directly determined by solving Eq. (3.2). This equation is an inhomogeneous partial differential equation that can be simplified by employing the decoupling coefficient given by Eq. (3.6).

Eq. (3.2) is normalized with respect to the permittivity in the x_2 direction.

$$\Psi_{3,11} + \frac{\beta^\sigma_{11}}{\beta^\sigma_{22}}\Psi_{3,22} = -\left(\frac{g_{211} + 2g_{112}}{\beta^\sigma_{22}}\right)\Phi_{,221} - \frac{g_{222}}{\beta^\sigma_{22}}\Phi_{,111} \tag{3.16}$$

It can be shown that particular solution given by Eq. (3.17) satisfies Eq. (3.16) when the decoupling ratio holds. The particular solution given by Eq. (3.17) was simplified using a different form of the piezoelectric coefficients (IEEE, 1987), $-g_{222}/\beta^\sigma_{22} = d_{222}$

$$\Psi^{\mathrm{p}}_3 = -d_{222}\Phi_{,1} \tag{3.17}$$

where the superscript p defines the particular component of the solution.

The homogeneous solution is found by setting Eq. (3.16) equal to zero and rescaling the coordinates using the following equations,

$$\bar{x}_1 = x_1 \tag{3.18}$$

$$\bar{x}_2 = bx_2 \tag{3.19}$$

$$b = \sqrt{\frac{\beta_{22}^{\sigma}}{\beta_{11}^{\sigma}}} \tag{3.20}$$

This gives Laplace's equation in the rescaled coordinate system where the superscript h defines the homogeneous component of the solution.

$$\nabla^2 \Psi_3^{\mathrm{h}} = 0 \tag{3.21}$$

To determine the electric displacement components, the homogeneous solution is rescaled to the original coordinate system and the particular solution is added to the final result.

$$\Psi_3 = \Psi_3^{\mathrm{h}} + \Psi_3^{\mathrm{p}} \tag{3.22}$$

The boundary conditions are then applied in the original coordinate system to determine the electric displacement components. The boundary conditions for the asymptotic crack problem will be given in Section 5.

4. Stroh's formalism

The Stroh formalism solves the governing equations by assuming a generalized two-dimensional displacement field that is a function of (x_1, x_2) only. The displacement field is introduced by utilizing a set of complex planes (z_j) where $i = 1$ to 3 for the two-dimensional case.

$$u_i = 2\mathrm{Re}\left\{ \sum_{j=1}^{3} A_{ij} f(z_j) q_j \right\} \tag{4.1}$$

$$z_j = x_1 + p_j x_2 \tag{4.2}$$

The complex coefficients A_{ij}, q_j, and p_j are constants to be determined.

The electric field is included in Eq. (4.1) by defining u_3 as the electric potential.

$$E_i = -u_{3,i} \tag{4.3}$$

The stress and electric displacement components are rewritten in matrix form to make use of the formulation developed by Stroh.

$$\Sigma_{i1} = \sigma_{i1} \quad \text{for } i = 1,2 \quad \text{and} \quad \Sigma_{i1} = D_1 \quad \text{for } i = 3 \tag{4.4}$$

$$\Sigma_{i2} = \sigma_{i2} \quad \text{for } i = 1,2 \quad \text{and} \quad \Sigma_{i2} = D_2 \quad \text{for } i = 3 \tag{4.5}$$

The stress tensor and electric displacement vector can be represented by a generalized vector potential, φ_i. By comparing Eqs. (2.2) and (2.8), the Airy stress potential and electric displacement potential can be related to the generalized stress vector potential.

$$\Sigma_{i1} = -\varphi_{i,2} = -\Phi_{,k2} \in_{ik3} \quad (i,k = 1,2) \tag{4.6}$$

$$\Sigma_{i2} = \varphi_{i,1} = \Phi_{,k1} \in_{ik3} \quad (i,k = 1,2) \tag{4.7}$$

$$\Sigma_{i1} = -\varphi_{i,2} = \Psi_{3,2} \quad (i = 3) \tag{4.8}$$

$$\Sigma_{i2} = \varphi_{i,1} = -\Psi_{3,1} \quad (i = 3) \tag{4.9}$$

The generalized vector potential can be related to the complex function given by Eq. (4.1) through substitution into the constitutive law, Eqs. (2.12a,b).

$$\varphi_i = 2\mathrm{Re}\left\{ \sum_{j=1}^{3} B_{ij} f(z_j) q_j \right\} \tag{4.10}$$

The complex constants, B_{ij}, are related to A_{ij} and material coefficients (Ting, 1996).

Upon substituting displacements and the electric potential into the constitutive relation, an eigenvector problem is developed by applying Eqs. (2.1) and (2.7).

$$(C^E_{ijkl} a_k + e_{kij} a_3)(\delta_{j1} + p\delta_{j2})(\delta_{l1} + p\delta_{l2}) = 0 \tag{4.11a}$$

$$(e_{ikl} a_k - \kappa^{\varepsilon}_{ik} a_3)(\delta_{i1} + p\delta_{i2})(\delta_{l1} + p\delta_{l2}) = 0 \tag{4.11b}$$

This provides a means for determining the eigenvectors, A_{ij}, and the eigenvalues, p_i. The eigenvectors, B_{ij}, are found through constitutive relations or reformulating the eigenvector problem to solve A_{ij}, B_{ij}, and p_i simultaneously (Ting, 1996).

The final form of the generalized stress potential given by Eq. (4.10) and the generalized displacement field given by Eq. (4.1) is written in terms of the Stroh eigenvectors (a_i, b_i), the complex function $(f(z_i))$, and a set of boundary condition constants (q_j). The eigenvectors are given in matrix form where only three of the six eigenvectors are utilized in the solution.

$$\mathbf{A} = [\,\mathbf{a}_1 \quad \mathbf{a}_2 \quad \mathbf{a}_3\,] \tag{4.12}$$

$$\mathbf{B} = [\,\mathbf{b}_1 \quad \mathbf{b}_2 \quad \mathbf{b}_3\,] \tag{4.13}$$

The solution utilizes three eigenvectors which are chosen to have positive imaginary components. The other three vectors are linear dependent in three-dimensional space; therefore, are not necessary to uniquely solve the problem (Stroh, 1958).

5. Fracture problem

Asymptotic crack tip fields are found using orthotropic rescaling and compared to the Stroh formalism. The crack is assumed to be contained within an infinite piezoelectric medium with impermeable crack faces. The origin of the coordinate system is located at the crack tip as shown in Fig. 1. A closed form solution is obtained for the stress and electric displacement fields using the orthotropic rescaling given by Eqs. (5.1) and (5.2) when $\rho' = 1$ and decoupling holds,

$$\begin{bmatrix} \sigma_{11} \\ \sigma_{12} \\ \sigma_{22} \end{bmatrix} = \frac{K_{\mathrm{I}}}{\sqrt{2\pi\tilde{r}}} \cos\left(\frac{\tilde{\theta}}{2}\right) \begin{bmatrix} a^2\left(1 - \sin\left(\frac{\tilde{\theta}}{2}\right)\sin\left(\frac{3\tilde{\theta}}{2}\right)\right) \\ a\sin\left(\frac{\tilde{\theta}}{2}\right)\cos\left(\frac{3\tilde{\theta}}{2}\right) \\ \left(1 + \sin\left(\frac{\tilde{\theta}}{2}\right)\sin\left(\frac{3\tilde{\theta}}{2}\right)\right) \end{bmatrix} \tag{5.1}$$

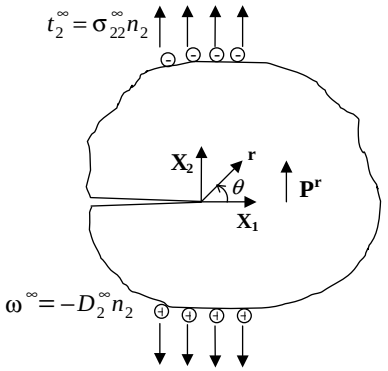

Fig. 1. Crack geometry used in the contour plots. A crack length of $2c = 10$ mm, constant radius of 100 μm around the crack tip are used in all plots.

$$\begin{bmatrix} D_1 \\ D_2 \end{bmatrix} = \begin{bmatrix} \frac{-bK_{IV}}{\sqrt{2\pi\tilde{r}}} \sin\left(\frac{\tilde{\theta}}{2}\right) + d_{222}\frac{K_I}{\sqrt{2\pi}}\left[\frac{b}{\sqrt{\tilde{r}}}\sin\left(\frac{\bar{\theta}}{2}\right) + \frac{a}{\sqrt{\tilde{r}}}\cos\left(\frac{\tilde{\theta}}{2}\right)\sin\left(\frac{\tilde{\theta}}{2}\right)\sin\left(\frac{3\tilde{\theta}}{2}\right)\right] \\ \frac{K_{IV}}{\sqrt{2\pi\bar{r}}}\cos\left(\frac{\bar{\theta}}{2}\right) + d_{222}\frac{K_I}{\sqrt{2\pi}}\left[\frac{1}{\sqrt{\bar{r}}}\cos\left(\frac{\bar{\theta}}{2}\right)\left\{1 + \sin\left(\frac{\bar{\theta}}{2}\right)\sin\left(\frac{3\bar{\theta}}{2}\right)\right\} - \frac{1}{\sqrt{\bar{r}}}\cos\left(\frac{\bar{\theta}}{2}\right)\right] \end{bmatrix} \tag{5.2}$$

where a and b are rescaling coefficients from Eqs. (3.12) and (3.20), d_{222} is the piezoelectric coefficient and $(\tilde{r}, \tilde{\theta})$ and $(\bar{r}, \bar{\theta})$ are the rescaled coordinate systems, and the strain and electric field are determined from the constitutive law. Details of the solution will be presently shown.

The definitions of stress and electric displacement intensity factors are given by,

$$K_I = \lim_{r\to 0}\sqrt{2\pi r}\sigma_{22}|_{\theta=0} \tag{5.3}$$

$$K_{IV} = \lim_{r\to 0}\sqrt{2\pi r}D_2|_{\theta=0} \tag{5.4}$$

It will be shown that the Mode I and Mode IV intensity factors are not affected by the coordinate rescaling, therefore standard solutions for Mode I intensity factors can be readily applied to Eq. (5.1) since stress is independent of applied electric fields. Special consideration must be taken to determine the Mode IV intensity factor. The center crack panel is a special case of decoupling, $K_{IV} = D_2^\infty\sqrt{\pi c}$, where D_2^∞ is the electric displacement applied at the far-field boundary and $2c$ is the crack length. This is not automatically satisfied in fracture problems with other geometries. Other crack geometries require determining the electric displacement at $\theta = 0°$ near the crack tip to determine K_{IV}. This can be achieved analytically for certain geometries, otherwise finite element analysis is typically employed.

5.1. Orthotropic rescaling details

5.1.1. Stress fields

The advantage of the orthotropic rescaling technique is that it allows existing isotropic elastic and isotropic dielectric solutions to be applied to orthotropic materials in the rescaled coordinate system. For special classes of piezoelectric material, the relations provided by the decoupling coefficient and $\rho' = 1$ results in the biharmonic equation. This constraint decouples applied electric field from affecting stress concentrations. The electric displacement is determined from the particular and homogeneous solution given in Section 3.2. The electric field is then determined from the constitutive law.

The stress components are presented first in terms of the rescaled coordinates and then scaled back to the original coordinate system. An "idealized" set of material properties is presented to show that stress contours from the orthotropic rescaling and the Stroh formalism are equivalent in this case. It is also shown that the electric field does not induce stress near the crack tip for the "idealized" case.

To apply the isotropic Mode I elasticity solution, the boundary conditions on the crack surface are evaluated in the rescaled coordinates. The following equations relate the rescaled coordinate plane $(\tilde{r},\tilde{\theta})$ to the original coordinates (x_1,x_2),

$$\tilde{r}^2 = x_1^2 + a^2 x_2^2 \tag{5.5a}$$

$$\tilde{\theta} = \tan^{-1}\left(\frac{a x_2}{x_1}\right) \tag{5.5b}$$

From Eq. (5.5b), $\tilde{\theta}$ and θ are equivalent at $\pm\pi$. This provides the necessary condition to satisfy the zero traction boundary condition on the crack surface.

The asymptotic stress fields are given in the rescaled coordinates for Mode I loading by analogy with the isotropic solution.

$$\begin{bmatrix}\sigma_{\tilde{1}\tilde{1}}\\ \sigma_{\tilde{1}\tilde{2}}\\ \sigma_{\tilde{2}\tilde{2}}\end{bmatrix} = \frac{K_{\mathrm{I}}}{\sqrt{2\pi\tilde{r}}}\cos\left(\frac{\tilde{\theta}}{2}\right)\begin{bmatrix}1-\sin\left(\frac{\tilde{\theta}}{2}\right)\sin\left(\frac{3\tilde{\theta}}{2}\right)\\ \sin\left(\frac{\tilde{\theta}}{2}\right)\cos\left(\frac{3\tilde{\theta}}{2}\right)\\ 1+\sin\left(\frac{\tilde{\theta}}{2}\right)\sin\left(\frac{3\tilde{\theta}}{2}\right)\end{bmatrix} \tag{5.6}$$

When the stress components are mapped back to the original (x_1,x_2) coordinate system, Eq. (5.1) is obtained.

The stress components in Eqs. (5.6) and (5.1) are written in terms of the Mode I stress intensity factor, K_{I}, which is identical to the isotropic definition of stress intensity, Eq. (5.3) when the rescaling factor is applied on the x_2 coordinate axis, as given by Eq. (5.5a). The stress components are shown to differ from the isotropic solution by the rescaling parameter, a. When the rescaling parameter, $a = 1$, the isotropic stress fields are recovered.

5.1.2. Electric displacement fields

The electric displacement components near a crack tip are determined for the limiting case of an impermeable crack. The homogeneous solution is first determined in terms of unknown constants and then the particular solution is added to the result. The unknown constant is determined by applying the impermeable crack face boundary conditions and Eq. (5.4). Since the stress concentration is decoupled from applied electrical loading, it is not necessary to obtain the stress solution simultaneously to determine the boundary condition constants.

Laplace's equation was obtained by rescaling the coordinate system according to Eqs. (3.18)–(3.20). The following equations relate the rescaled coordinate plane $(\bar{r},\bar{\theta})$ to the original coordinates (x_1,x_2),

$$\bar{r}^2 = x_1^2 + b^2 x_2^2 \tag{5.7a}$$

$$\bar{\theta} = \tan^{-1}\left(\frac{b x_2}{x_1}\right) \tag{5.7b}$$

The homogeneous component of the electric displacement potential is found using a complex potential,

$$\Psi_{\bar{3}}^{\mathrm{h}} = -C\bar{z}^{\lambda+1} = -(A_\lambda + \mathrm{i}B_\lambda)\bar{r}^{\lambda+1}\mathrm{e}^{(\lambda+1)\bar{\theta}} \tag{5.8}$$

where $\bar{z} = \bar{x}_1 + \mathrm{i}\bar{x}_2 = \bar{r}[\cos(\bar{\theta}) + \mathrm{i}\sin(\bar{\theta})]$.

The homogeneous components of the electric displacement are given in polar coordinates by the following equations,

$$D_{\bar{r}}^{\mathrm{h}} = \mathrm{Re}\left\{ \frac{1}{\bar{r}} \frac{\partial \Psi_3^{\mathrm{h}}}{\partial \bar{\theta}} \right\} = (\lambda+1)\bar{r}^{\lambda}\{A_\lambda \sin[(\lambda+1)\bar{\theta}] + B_\lambda \cos[(\lambda+1)\bar{\theta}]\} \tag{5.9}$$

$$D_{\bar{\theta}}^{\mathrm{h}} = -\mathrm{Re}\left\{ \frac{\partial \Psi_3^{\mathrm{h}}}{\partial \bar{r}} \right\} = (\lambda+1)\bar{r}^{\lambda}\{A_\lambda \cos[(\lambda+1)\bar{\theta}] - B_\lambda \sin[(\lambda+1)\bar{\theta}]\} \tag{5.10}$$

The particular solution must be added prior to applying the boundary conditions. The total electric displacement is given in the real coordinate system by the following equations by using Eqs. (2.8) and (3.17). For brevity, the field components are given in terms of Cartesian coordinates.

$$D_1 = D_1^{\mathrm{h}} + D_1^{\mathrm{p}} = D_1^{\mathrm{h}} + d_{222}\sigma_{12} \tag{5.11}$$

$$D_2 = D_2^{\mathrm{h}} + D_2^{\mathrm{p}} = D_2^{\mathrm{h}} + d_{222}\sigma_{22} \tag{5.12}$$

The impermeable crack is defined by setting $D_\theta|_{\theta=\pm\pi} = D_2|_{\theta=\pm\pi} = 0$. The particular solution is zero on the crack face ($\sigma_{22}|_{\theta=\pm\pi} = 0$), therefore only the homogeneous solution is needed to determine the unknown constants, A_λ and B_λ.

The asymptotic solution is found by ensuring finite electrical energy density and infinite electric displacement at the crack tip. This requires $\lambda = -1/2$ and $B_\lambda = 0$. The constant, A_λ, is determined by using the boundary condition given by Eq. (5.4).

$$D_2|_{\theta=0} = \frac{K_{\mathrm{IV}}}{\sqrt{2\pi r}} = \frac{A_\lambda}{2\sqrt{r}} + d_{222}\frac{K_{\mathrm{I}}}{\sqrt{2\pi r}} \tag{5.13}$$

$$A_\lambda = \sqrt{\frac{2}{\pi}}(K_{\mathrm{IV}} - d_{222}K_{\mathrm{I}}) \tag{5.14}$$

The electric displacement components can be written in terms of the stress intensity factors and a function of the two sets of rescaled coordinates, $(\tilde{r},\tilde{\theta})$ and $(\bar{r},\bar{\theta})$ as previously given by Eq. (5.2).

Both rescaled coordinate systems were used in determining the electric displacement field quantities near the crack tip. The electric displacement in the x_2 direction decouples from the Mode I stress intensity directly in front of the crack tip as defined in Eq. (5.13).

5.2. Stroh approach

Asymptotic field solutions around a crack tip are determined using the Stroh formalism. The governing equations developed by Stroh furnish the relations for creating a numerical algorithm to determine the eigenvalues and eigenvectors for a given set of material parameters. Detailed numerical results of the eigenvalue problem are given in Appendix A. The eigenvectors are used together with a complex function and boundary conditions constants to determine the stress fields.

The complex function used in Eqs. (4.1) and (4.10) must be determined to find the field quantities around a crack tip. The function must ensure finite strain energy and infinite stress and electric displacement at the crack tip. The following function satisfies these constraints in the electro-elastic body.

$$f(z_j) = \sqrt{z_j} \tag{5.15}$$

The unknown vector quantity, q_j, given in Eqs. (4.1) and (4.10) is found in order to satisfy the boundary conditions. This vector consists of three components for two-dimensional in-plane piezoelectric problems. Since an asymptotic crack solution is utilized, an assumption about the electric boundary condition is made

to simplify the analysis. An electrically impermeable crack is assumed (a limiting case, McMeeking, 1999) so that electric field concentration effects are captured near the crack tip. The following boundary conditions are utilized on the crack face.

$$\sigma_{ji}n_i = 0 \tag{5.16a}$$

$$D_i n_i = 0 \tag{5.16b}$$

The three boundary condition constants are complex; therefore, six equations are required to find both the real and imaginary components. According to Sih et al. (1965) the stress intensity factor applied to an isotropic material is equivalent to that in an orthotropic material. Suo et al. (1992) extended this relation to piezoelectric material. Based on their results, Eqs. (5.17a) and (5.17b) are used to uniquely solve the boundary condition constants for Mode I and Mode IV loading. When the material is under symmetrical loading (Mode I and IV), an additional boundary condition for no rotation is applied ahead of the crack tip, (5.17c).

$$\sigma_{22}|_{\theta=0} = \frac{K_{\mathrm{I}}}{\sqrt{2\pi r}} \tag{5.17a}$$

$$D_2|_{\theta=0} = \frac{K_{\mathrm{IV}}}{\sqrt{2\pi r}} \tag{5.17b}$$

$$u_2|_{\theta=0} = 0 \tag{5.17c}$$

The field quantities near the crack tip are given below in terms of the eigenvector solution,

$$\begin{bmatrix} u_1 \\ u_2 \\ \phi \end{bmatrix} = 2\mathrm{Re}\left\{ \begin{bmatrix} A_{11}q_1\sqrt{z_1} + A_{12}q_2\sqrt{z_2} + A_{13}q_3\sqrt{z_3} \\ A_{21}q_1\sqrt{z_1} + A_{22}q_2\sqrt{z_2} + A_{23}q_3\sqrt{z_3} \\ A_{31}q_1\sqrt{z_1} + A_{32}q_2\sqrt{z_2} + A_{33}q_3\sqrt{z_3} \end{bmatrix} \right\} \tag{5.18}$$

$$\begin{bmatrix} \sigma_{21} \\ \sigma_{22} \\ D_2 \end{bmatrix} = \mathrm{Re}\left\{ \begin{bmatrix} B_{11}q_1/\sqrt{z_1} + B_{12}q_2/\sqrt{z_2} + B_{13}q_3/\sqrt{z_3} \\ B_{21}q_1/\sqrt{z_1} + B_{22}q_2/\sqrt{z_2} + B_{23}q_3/\sqrt{z_3} \\ B_{31}q_1/\sqrt{z_1} + B_{32}q_2/\sqrt{z_2} + B_{33}q_3/\sqrt{z_3} \end{bmatrix} \right\} \tag{5.19}$$

$$\begin{bmatrix} \sigma_{11} \\ \sigma_{21} \\ D_1 \end{bmatrix} = -\mathrm{Re}\left\{ \begin{bmatrix} B_{11}q_1p_1/\sqrt{z_1} + B_{12}q_2p_2/\sqrt{z_2} + B_{13}q_3p_3/\sqrt{z_3} \\ B_{21}q_1p_1/\sqrt{z_1} + B_{22}q_2p_2/\sqrt{z_2} + B_{23}q_3p_3/\sqrt{z_3} \\ B_{31}q_1p_1/\sqrt{z_1} + B_{32}q_2p_2/\sqrt{z_2} + B_{33}q_3p_3/\sqrt{z_3} \end{bmatrix} \right\} \tag{5.20}$$

Eqs. (5.19) and (5.20) are compared to the closed form solutions determined by the orthotropic rescaling technique in the following section. Exact solutions are found when decoupling holds and $\rho' = 1$. Differences in the field quantities are compared using material coefficients for TRS600. [1]

6. Comparison of results

The orthotropic rescaling technique is directly compared to the Stroh formalism by evaluating changes in computed field quantities with respect to changes in material properties. The results are com-

[1] TRS Ceramics, Inc. State College, PA.

pared using an "idealized" set of material properties that satisfy the decoupling ratio and $\rho' = 1$; and a real set of material properties with ratios that do not satisfy the decoupling ratio and $\rho' = 1$. In addition, a parametric study illustrates differences in maximum principal stress when the decoupling ratio is greater or less than the ideal value. Contour plots are shown which plot stress components around the crack tip over a constant radius. Vector plots are used to compare electric displacement and electric fields near the crack tip.

The material properties employed in the analysis are based on TRS600. Material coefficients, s_{66}^D, g_{16}, and β_{11}^σ, were adjusted to satisfy the necessary ratios that gives the biharmonic equation. The material properties used in the orthotropic rescaling technique are given in Table 1. These coefficients were converted to the effective plane strain coefficients for direct comparison to the Stroh formalism, see Appendix A for details. The poling axis for the material is the x_2 direction.

Since the Stroh formalism uses another form of the constitutive law, the material coefficients given in Table 1 are computed in terms of the coefficients given by Eqs. (2.12a,b). The equivalent material properties are found in Table 2.

Contour plots representing the stress components around the crack tip are first given for the "idealized" case and then compared to the "real" case. The angular dependence on stress is plotted over a region of constant radius and crack orientation as shown in Fig. 1. Traction and surface charge are applied at the

Table 1
Piezoelectric material properties (plane strain coefficients) used to plot stress fields using the orthotropic rescaling technique

TRS600	ACTUAL	"IDEALIZED"
β_{22}^σ (V^2/N)	2.72×10^{7}	2.72×10^{7}
β_{11}^σ (V^2/N)	2.54×10^{7}	3.74×10^{7}
g_{22} (m^2/C)	0.0167	0.0167
g_{21} (m^2/C)	−0.0128	−0.0128
g_{16} (m^2/C)	0.0216	0.0318
s_{11}^D (m^2/N)	9.49×10^{-12}	9.49×10^{-12}
s_{22}^D (m^2/N)	8.27×10^{-12}	8.27×10^{-12}
s_{12}^D (m^2/N)	-3.94×10^{-12}	-3.94×10^{-12}
s_{66}^D (m^2/N)	2.66×10^{-11}	2.34×10^{-11}
$\beta_{11}^\sigma/\beta_{22}^\sigma$	0.78	1.14
$(g_{211}+g_{16})/g_{222}$	0.53	1.14
ρ'	0.92	1.00

The material coefficients (s_{66}^D, g_{16}, and β_{11}^σ) have been adjusted to meet the necessary ratios given by the decoupling coefficient and $\rho' = 1$. The decoupling ratio has been given for the plane strain case.

Table 2
Material properties related to the coefficients in Table 1 which are used to calculate stress fields using the Stroh formalism

TRS600	ACTUAL	"IDEALIZED"
κ_{22}^ε (N/V^2)	1.44×10^{-8}	1.44×10^{-8}
κ_{11}^ε (N/V^2)	2.33×10^{-8}	1.24×10^{-8}
e_{22} (C/m^2)	30.38	30.38
e_{21} (C/m^2)	−3.73	−3.73
e_{16} (C/m^2)	18.89	16.85
c_{11}^E (N/m^2)	8.16×10^{10}	8.16×10^{10}
c_{22}^E (N/m^2)	5.97×10^{10}	5.97×10^{10}
c_{12}^E (N/m^2)	3.20×10^{10}	3.20×10^{10}
c_{66}^E (N/m^2)	2.22×10^{10}	1.98×10^{10}

The material coefficients (c_{66}^E, e_{16} and κ_{11}^ε) correspond to the coefficients that were adjusted in Table 1.

far-field boundary in the x_2 direction. Mode I and Mode IV intensity factors are applied by letting $K_I = 1$ MPa $\sqrt{m}$ and $K_{IV} = 0.001$ C/m^2 $\sqrt{m}$.

Fig. 2 depicts the crack tip stress field for the maximum principal stress in the "idealized" piezoelectric material. The plot includes the isotropic solution for comparison to the orthotropic material behavior. The stress contour under applied surface charge was not included since it had no effect on the stress fields for the "idealized" case. The orthotropic rescaling technique and Stroh's formalism give identical stress fields.

Fig. 3 represents how the orthotropic rescaling was less accurate when the actual material properties for TRS600 were used with Eq. (5.1). The isotropic solution is not included in the figure. Since the electric field is no longer decoupled from the stress field, the effect of surface charge is included in Fig. 3 by use of the Stroh formalism. The largest deviation from the exact solution was directly ahead of the crack tip. The lower accuracy of stress ahead of the crack tip was determined to emanate from the stress components σ_{11}.

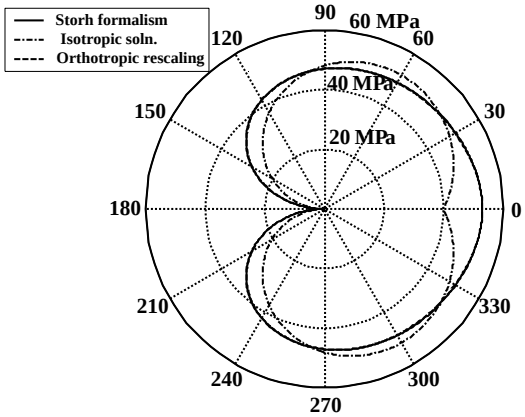

Fig. 2. Stress contour around the crack tip for the maximum principal stress, σ_1, from $\theta = \pi$ to $\theta = -\pi$ when $r = 100$ μm when rescaling conditions are met.

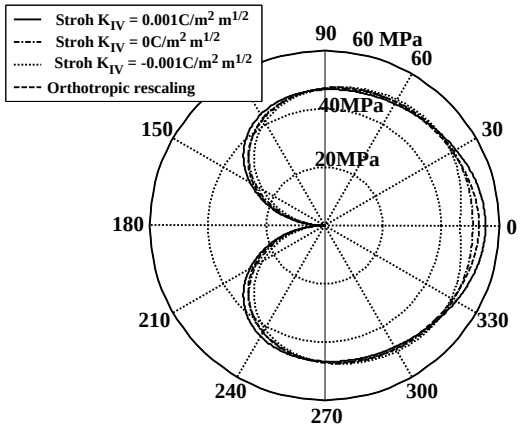

Fig. 3. Resulting stress contour for the maximum principal stress, σ_1, when the actual material parameters are used; $\theta = \pi$ to $\theta = -\pi$ when $r = 100$ μm.

The effects of the decoupling coefficient are illustrated in Fig. 4. The maximum principal stress is shown to change when the permittivity ratio deviates from the "idealized" value if the material is under both Mode I and Mode IV loading. In the example, $K_{\mathrm{I}} = 1$ MPa $\sqrt{\mathrm{m}}$ and $K_{\mathrm{IV}} = 0.002$ C/m^2 $\sqrt{\mathrm{m}}$ was used. If the permittivity ratio is greater than the "idealized" case, the maximum principal stress increases directly ahead of the crack tip. Conversely, if the ratio decreases, the maximum principal stress decreases ahead of the crack tip.

The changes in stress directly ahead of the crack tip can be described by the amount of electric displacement permitted by the dielectric constant (β^{σ}_{11}). As the permittivity constant in the x_1 direction increases, the electric field drives more strain in this direction causing an incompatibility. The strain incompatibility is compensated by larger stresses in the x_1 direction (σ_{11}) which alters the maximum principal stress at this point. A converse argument can be made when the permittivity coefficient decreases below the "idealized" case.

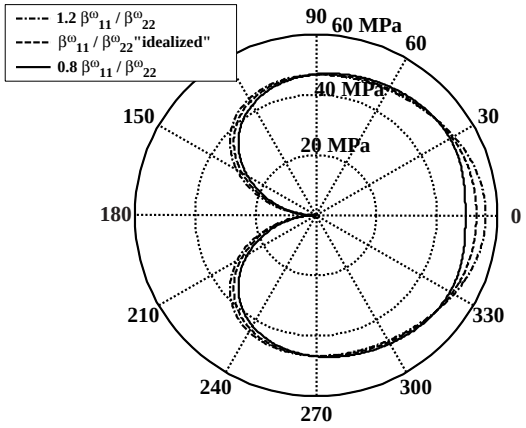

Fig. 4. Parametric study of the effects of the decoupling ratio on the maximum principal stress (σ_1) near the crack tip when $K_{\mathrm{IV}} = 0.002$ C/m^2 $\sqrt{\mathrm{m}}$. The decoupling ratio, $\beta^{\sigma}_{11}/\beta^{\sigma}_{22}$, was modified while holding the piezoelectric coefficients constant.

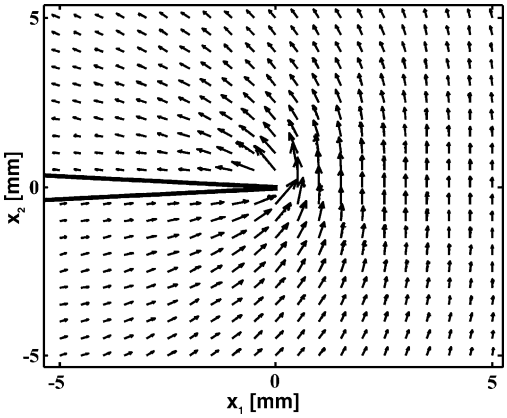

Fig. 5. Vector plot of electric displacement for TRS600 material properties under Mode I and Mode IV loading ($K_{\mathrm{I}} = 1$ MPa $\sqrt{\mathrm{m}}$, $K_{\mathrm{IV}} = 0.001$ C/m^2 $\sqrt{\mathrm{m}}$). The solutions are practically identical. The Stroh formalism is shown by dotted arrows; the orthotropic rescaling result is shown by solid arrows.

The electric displacement is evaluated under a combined Mode I and Mode IV loading ($K_I = 1$ MPa $\sqrt{m}$ and $K_{IV} = 0.001$ C/m^2 $\sqrt{m}$). A vector plot is used to represent the direction of electric displacement in a confined region near the crack tip. The remnant polarization is not included in the plots. The crack tip is drawn on the plot as a reference point. Exact correlation was found for the electric displacement and electric field when using "idealized" material properties. Fig. 5 qualitatively represent how the piezoelectric material responds to electro-mechanical loading for TRS600. Negligible differences in electric displacement were observed. Similar results were found for the electric field components.

7. Concluding remarks

A generalized form of the Airy stress potential was used to formulate closed form solutions for linear piezoelectric boundary value problems. A new technique using orthotropic rescaling was presented which identified certain ratios of elastic, piezoelectric, and dielectric material coefficients necessary to reduce the formulation to the biharmonic equation. Previously solved isotropic elasticity solutions were utilized to determine stress fields near the crack tip.

The orthotropic rescaling technique was verified using Stroh's formalism for an "idealized" set of material coefficients. The orthotropic rescaling technique gives exact correlation to Stroh's method for the "idealized" set of material coefficients. The technique was less accurate when an actual set of material properties was employed, although reasonable estimations were achieved under mechanical loading. The stress fields from the rescaling technique should be avoided when large electrical loading is present. Considerable deviations in stress were observed directly ahead of the crack tip when a surface charge was present.

The electric displacement and electric field determined from orthotropic rescaling matched well with the Stroh formalism under electro-mechanical loading for the "idealized" case and for TRS600 material properties. The orthotropic rescaling appears to be a robust technique for determining electric field and electric displacement components near a crack tip.

The decoupling coefficient was shown to influence the stress components near a crack tip, although for a certain ratio of piezoelectric and dielectric coefficients, the stress components are independent of an applied electric field.

Acknowledgements

Notes and discussions with Professor Robert McMeeking at the University of California, Santa Barbara and Professor Jianmin Qu at the Georgia Institute of Technology were of immense help in this work and greatly appreciated. The authors would also like to acknowledge their appreciation for the support of Dr. Wes Hackenburger and Paul Rehrig of TRS Ceramics, State College PA and of AFOSR through grant, F49620-02-1-0030. Support through ARO grant DAAD 19-02-1-0241 is gratefully appreciated.

Appendix A

A.1. Plane strain coefficients

A set of plane strain coefficients were used to directly compare the orthotropy rescaling technique to the Stroh formalism. The coordinate axis is assumed to be aligned with the material coordinates. For transverse

isotropic piezoelectric materials poled in the two direction, the constitutive law is written in the following form.

$$\begin{bmatrix}\gamma_1\\ \gamma_2\\ \gamma_3\\ \gamma_4\\ \gamma_5\\ \gamma_6\end{bmatrix} = \begin{bmatrix} s_{11}^D & s_{12}^D & s_{13}^D & 0 & 0 & 0\\ s_{12}^D & s_{22}^D & s_{12}^D & 0 & 0 & 0\\ s_{13}^D & s_{12}^D & s_{11}^D & 0 & 0 & 0\\ 0 & 0 & 0 & s_{66}^D & 0 & 0\\ 0 & 0 & 0 & 0 & s_{55}^D & 0\\ 0 & 0 & 0 & 0 & 0 & s_{66}^D \end{bmatrix} \begin{bmatrix}\sigma_1\\ \sigma_2\\ \sigma_3\\ \sigma_4\\ \sigma_5\\ \sigma_6\end{bmatrix} + \begin{bmatrix} 0 & g_{21} & 0\\ 0 & g_{22} & 0\\ 0 & g_{21} & 0\\ g_{16} & 0 & 0\\ 0 & 0 & 0\\ 0 & 0 & g_{16}\end{bmatrix} \begin{bmatrix}D_1\\ D_2\\ D_3\end{bmatrix} \tag{A.1}$$

$$\begin{bmatrix}E_1\\ E_2\\ E_3\end{bmatrix} = -\begin{bmatrix} 0 & 0 & 0 & 0 & 0 & g_{16}\\ g_{21} & g_{22} & g_{21} & 0 & 0 & 0\\ 0 & 0 & 0 & g_{16} & 0 & 0\end{bmatrix} \begin{bmatrix}\sigma_1\\ \sigma_2\\ \sigma_3\\ \sigma_4\\ \sigma_5\\ \sigma_6\end{bmatrix} + \begin{bmatrix} \beta_{11}^\sigma & 0 & 0\\ 0 & \beta_{22}^\sigma & 0\\ 0 & 0 & \beta_{11}^\sigma\end{bmatrix} \begin{bmatrix}D_1\\ D_2\\ D_3\end{bmatrix} \tag{A.2}$$

The following effective elastic constants were used in the orthotropic rescaling for the plane strain problem, where the plane of interest is (x_1, x_2). All other material coefficients were equivalent to the plane stress case.

$$s_{11}^{D'} = s_{11}^D - \frac{s_{13}^D s_{13}^D}{s_{11}^D} \tag{A.3}$$

$$s_{22}^{D'} = s_{22}^D - \frac{s_{12}^D s_{12}^D}{s_{11}^D} \tag{A.4}$$

$$s_{12}^{D'} = s_{12}^D - \frac{s_{12}^D s_{13}^D}{s_{11}^D} \tag{A.5}$$

$$g'_{22} = g_{22} - \frac{s_{12}^D}{s_{11}^D} g_{21} \tag{A.6}$$

$$g'_{21} = g_{21} - \frac{s_{13}^D}{s_{11}^D} g_{21} \tag{A.7}$$

$$\beta_{22}^{\sigma'} = \beta_{22}^\sigma + \frac{g_{21} g_{21}}{s_{11}^D} \tag{A.8}$$

A.2. Stroh eigensolution

The Stroh eigenvalues/eigenvectors are presented for both the "idealized" case and real set of material properties used in the analysis. For the decoupled case, a degeneracy exists where two of the eigenvalues/eigenvectors are repeated. The boundary condition constants (corresponding to $K_{\mathrm{I}} = 1$ MPa $\sqrt{\mathrm{m}}$ and $K_{\mathrm{IV}} = 0.001$ C/m^2 $\sqrt{\mathrm{m}}$) is included in the boundary condition constants.

Idealized properties:

$$\begin{aligned} p_1 &= 1.152\mathrm{i} \\ p_2 &= 1.152\mathrm{i} \\ p_3 &= 0.935\mathrm{i} \end{aligned} \tag{A.9}$$

$$\mathbf{A} = \begin{bmatrix} -1.51\mathrm{i} \times 10^{-11} & -1.51\mathrm{i} \times 10^{-11} & 36.48\mathrm{i} \times 10^{-11} \\ 1.25 \times 10^{-11} & 1.25 \times 10^{-11} & 50.90 \times 10^{-11} \\ 0.01 & 0.01 & -1.00 \end{bmatrix} \tag{A.10}$$

$$\mathbf{B} = \begin{bmatrix} 0.76 & 0.76 & (-5.30 + 2.20\mathrm{i}) \times 10^{-13} \\ 0.66\mathrm{i} & 0.66\mathrm{i} & (-2.40 - 5.80\mathrm{i}) \times 10^{-13} \\ 3.34\mathrm{i} \times 10^{-10} & 3.34\mathrm{i} \times 10^{-10} & -2.86 \times 10^{-8} \end{bmatrix} \tag{A.11}$$

$$\mathbf{q} = \begin{bmatrix} (96.80 + 6.17\mathrm{i}) \times 10^{11} \\ (-96.80 - 6.17\mathrm{i}) \times 10^{11} \\ 9.14 \times 10^{-6} - 6.86\mathrm{i} \times 10^{3} \end{bmatrix} \tag{A.12}$$

Actual material properties:

$$\begin{aligned} p_1 &= -0.31 + 1.06\mathrm{i} \\ p_2 &= 0.31 + 1.06\mathrm{i} \\ p_3 &= 1.23\mathrm{i} \end{aligned} \tag{A.13}$$

$$\mathbf{A} = \begin{bmatrix} (0.26 - 1.44\mathrm{i}) \times 10^{-11} & (-0.26 - 1.44\mathrm{i}) \times 10^{-11} & -0.73\mathrm{i} \times 10^{-11} \\ (1.26 - 0.28\mathrm{i}) \times 10^{-11} & (1.26 + 0.28\mathrm{i}) \times 10^{-11}\mathrm{i} & 0.27 \times 10^{-11} \\ 0.01 - 0.01\mathrm{i} & 0.01 + 0.01\mathrm{i} & 0.027 \end{bmatrix} \tag{A.14}$$

$$\mathbf{B} = \begin{bmatrix} 0.74 & 0.74 & 0.78 \\ 0.19 + 0.64\mathrm{i} & -0.19 + 0.64\mathrm{i} & 0.63\mathrm{i} \\ (-0.93 + 3.45\mathrm{i}) \times 10^{-10} & (0.93 + 3.45\mathrm{i}) \times 10^{-10} & -3.38 \times 10^{-10} \end{bmatrix} \tag{A.15}$$

$$\mathbf{q} = \begin{bmatrix} (9.67 - 4.33\mathrm{i}) \times 10^{5} \\ (-9.67 - 4.33\mathrm{i}) \times 10^{5} \\ -7.42 \times 10^{-10} + 8.27\mathrm{i} \times 10^{5} \end{bmatrix} \tag{A.16}$$

References

IEEE Standard on Piezoelectricity, 1987. The Institute of Electrical and Electronics Engineers, Inc., New York, NY.

Kamlah, M., 2001. Ferroelectric and ferroelastic piezoceramics-modeling of electromechanical hysteresis phenomena. Continuum Mech. Thermodyn. 13, 219–268.

Malvern, L.E., 1969. Introduction to the Mechanics of a Continuous Medium. Prentice-Hall, Inc., Up Saddle River, NJ.

McMeeking, R.M., 1999. Crack tip energy release rate for a piezoelectric compact tension specimen. Eng. Fract. Mech. 64, 217–244.

Pak, Y., 1992. Linear electro-elastic fracture mechanics of piezoelectric materials. Int. J. Fract. 54, 79–100.
Sih, G.C., Paris, P.C., Irwin, G.R., 1965. On cracks in rectilinearly anisotropic bodies. Int. J. Fract. Mech. 1, 189–203.
Sosa, H., 1990. Plane problems in piezoelectric media with defects. Int. J. Solids Struct. 28 (4), 491–505.
Stroh, A.N., 1958. Dislocations and cracks in anisotropic elasticity. Philos. Mag. 7, 625–646.
Suo, Z., Bao, G., Fan, B., Wang, T.C., 1991. Orthotropy rescaling and implications for fracture in composites. Int. J. Solids Struct. 28 (2), 235–248.
Suo, Z., Kuo, C.-M., Barnett, D.M., Willis, J.R., 1992. Fracture mechanics for piezoelectric ceramics. J. Mech. Phys. Solids 40 (4), 739–765.
Ting, T.C.T., 1996. Anisotropic Elasticity. Oxford University Press, New York.
Weber, C., 1948. Spannungsfunktioen des dreidimensionalen Kontinuums. Z. Angew. Math. Mech. 28 (7/8), 193–197.
Zhang, T.-Y., Zhao, M., Tong, P., 2001. Fracture of piezoelectric ceramics. Adv. Appl. Mech. 38, 147–289.